Research Article **Kenkyu Journal of Nanotechnology & Nanoscience** **ISSN: 2455-183X**

Citation: Pal M, Bera S, Khan H and Jana S * (2015) Effect of Ga doping on Microstructural, Optical and Photocatalytic Properties of Nanostructured Zinc Oxide Thin Films 1:100109

Effect of Ga doping on Microstructural, Optical and Photocatalytic Properties of Nanostructured Zinc Oxide Thin Films

Pal M, Bera S, Khan H and Jana S *

Sol-Gel Division, CSIR-Central Glass and Ceramic Research Institute (CSIR-CGCRI), 196, Raja S. C. Mullick Road, P.O.- Jadavpur University, Kolkata-700032, India.

Abstract

Ga doped nanostructured zinc oxide thin films (thickness, 160-170 nm) on pure silica glass substrate were prepared from zinc acetate based precursor solutions by varying Ga doping level (0 to 6%). The presence of nanocrystalline hexagonal ZnO was confirmed by X-ray diffraction study whereas the field emission scanning and transmission electron microscopic analyses evidenced the existence of quasi-spherical ZnO with a decreased trend in crystallite/particle size vis-à-vis an enhancement of direct band gap energy of the films on increasing the doping level. Root means square (RMS) film surface roughness was determined by atomic force microscope and found maximum RMS roughness value in 1% doped film. Photoluminescence (PL) emission spectral study revealed the formation of various intrinsic/extrinsic defects along with the presence of characteristics band edge emission of ZnO at ~ 385 nm (UVPL). However, a lowest relative intensity of the UVPL emission was found in 1% doped film (G1ZO), indicating an appreciable decrease in the recombination rate of photogenerated charge carriers in the semiconductor. The photocatalytic activity of the films towards degradation of rhodamine 6G dye was performed under UV (254 nm) and obtained the maximum value of dye degradation rate constant (considering first order reaction kinetics) in 1% doped film (G1ZO). On increasing doping level, the trend in change of defect concentration (oxygen vacancies) as analyzed by Raman spectral study was found identical with the dye photodegradation activity of the films. The G1ZO film would expect to decompose micro-organisms even under exposure of visible light.

Keywords: Nanostructured ZnO thin film; Sol-gel technique; Band gap energy; Raman spectra; Photoluminescence spectra; Oxygen deficiency; Photocatalyst; Organic dye.

***Corresponding Authors:** Sol-Gel Division, CSIR-Central Glass and Ceramic Research Institute (CSIR-CGCRI), Kolkata, 700032, India, Tel: +91-33-2483 8082, + 91-9432355818, Email: sjana@cgcri.res.in, janasunirmal@hotmail.com

Received: October 24, 2015; **Accepted:** November 14, 2015; **Published:** November 16, 2015

Citation: Pal M, Bera S, Khan H and Jana S * (2015) Effect of Ga doping on Microstructural, Optical and Photocatalytic Properties of Nanostructured Zinc Oxide Thin Films 1:100109

Introduction

With the growth of industries, the environment pollution becomes a serious problem globally. Nanostructured metal oxide semiconductor (MOS) [1] as photocatalyst would solve the problem economically and efficiently. The MOS could decompose organic pollutants like dyes, detergents, pesticides, volatile organic compounds under exposure of suitable light. ZnO is a wide band gap (3.3 eV) n-type MOS with large exciton binding energy (60 meV). It could be used as an electrical, optical and optoelectronic material. It is worthy to note that the doping of group IIIA elements (such as B, Al and Ga) in the periodic table, electrical conductivity of ZnO film could be improved without major sacrifice of optical transparency in the visible region [2]. This makes the thin film very useful in flat panel displays, photovoltaic, electrochromic and solar cells applications. In addition, ZnO is a non-toxic, biocompatible and inexpensive material [3]. Doping in ZnO by p or d block elements consequences substantial changes in their structural, optical, electrical and optoelectronic properties including photocatalytic activity of the material and the change of lattice parameters and defects (intrinsic/extrinsic) concentration in the crystal lattice could depend upon the nature and level of doping [4-9]. However, the doping level primarily depends on the crystal size and in this respect, the formation of several defects in ZnO has been recognized both theoretically and experimentally [10-12]. These defects could form individual energy level within the band gap of ZnO. It is also known that the efficiency of a photocatalyst could be improved by creating oxygen vacancies that could function as electron acceptors [13]. However, many defects could able to trap photogenerated charge carriers (electrons and holes) which could diminish the electron and hole recombination rate, the great parameter for enhancing the photocatalytic activity of a semiconductor. In addition, surface morphology and surface roughness [14] would play an important role for the improvement of the photocatalytic activity. In this respect, we reported previously, the influence of defect concentration on the photocatalytic activity of Al doped ZnO sol-gel based thin films by varying doping concentration [15]. It is known that sol-gel is a facile and cost effective technique where film crystallinity, morphology and optical properties depend upon several factors such as sol/solution chemistry, dopant content and nature, curing condition [16]. It is also true that the Ga doped ZnO thin films (GZO) has exceptional optical and electrical properties that would be due its low reactivity to oxygen and comparable ionic radius of Ga (III) (0.62 Å) to Zn (II) (0.72 Å) [17]. However, the effect of defect concentration particularly oxygen vacancies seemed not studied earlier especially in sol-gel based Ga doped ZnO thin films. Moreover, no report is yet found on the photocatalytic study of Ga doped zinc oxide films.

Thus, the present work highlights an influence of Ga doping on structural, optical and photocatalytic properties of sol-gel based ZnO thin films deposited from the precursor solutions with varying Ga doping level. The thin films were characterized to examine their crystallinity, microstructure and morphology as well as their optical property and photocatalytic

Received: October 24, 2015; **Accepted:** November 14, 2015; **Published:** November 16, 2015

Citation: Pal M, Bera S, Khan H and Jana S * (2015) Effect of Ga doping on Microstructural, Optical and Photocatalytic Properties of Nanostructured Zinc Oxide Thin Films 1:100109

activity. Finally, we correlated the properties to the photocatalytic activity of the thin films towards decomposition of an organic dye (rhodamine 6G).

Materials and methods

Preparation of precursor solutions and thin films

The entire chemicals were used without their further purifications. The precursor solutions for Ga doped zinc oxide thin films were prepared from zinc acetate dihydrate ($Zn(CH_3COO)_2.2H_2O$, ZA, Sigma Aldrich, purity 98%) and gallium nitrate hydrate (Alfa Aesar, purity 99.9%) as the sources of Zn and Ga, respectively. The mixed solvent, iso-propanol (IP, for synthesis, Merck) and double distilled water (DDW; IP : DDW = 1.37 to 1.43, weight ratio) along with acetylacetone (acac, Merck, 98%; ZA : acac = 1 : 1, mol ratio) as solution stabilizer were used in the precursor. The content of Ga was varied from 0 to 6 atomic percent (at.%) with respect to Zn. However, the total oxide content was kept fixed to 6 weight percent (wt.%) in all the solutions. It should be mentioned that the adherence of as-prepared solutions to the pure silica glass (Suprasil grade, Heraus, Germany, dimensions: 25 mm x 10 mm x 1 mm) used for the thin films deposition was very poor. However, after ageing the solutions for ~7 days a good adherence to the cleaned substrate was observed. The solutions with the Ga contents 0, 1, 2, 4 and 6% were designated as SG0ZO, SG1ZO, SG2ZO, SG4ZO and SG6ZO, respectively.

In this work, pure silica glass (Suprasil grade, Heraus, Germany, dimensions: 25 mm x 10 mm x 1 mm) was used for deposition of Ga doped ZnO (GZO) thin films. The GZO films were deposited using the aged precursor solutions on cleaned silica glass substrate by dip coating technique (Dip Master 200, Chemat Technology Inc., USA) with a fixed withdrawal speed of 12 cm/min. However, to obtain the oxide films, the as-deposited samples were initially dried in an air oven at 60^{o}C followed by thermal curing at 500^{o}C for 1 h soaking time under air atmosphere in an electrical furnace. The final films derived from the aged precursor solutions, SG0ZO, SG1ZO, SG2ZO, SG4ZO and SG6ZO were designated as G0ZO, G1ZO, G2ZO, G4ZO and G6ZO, respectively. It is noted that the details of precursor solution preparation, cleaning of glass substrate and deposition of films had been discussed in our previous report [15].

Characterizations

The crystal phase and crystallite size of ZnO in the thin films were determined by employing an X-ray diffractometer (Rigaku Smart Lab) with CuKα radiation (1.5406Å) operating at 9 kW in the diffraction angle (2θ), 20 to 70^o. The crystallite size of zinc oxide was calculated using Scherrer's equation and the lattice parameters of ZnO crystal were calculated from the XRD patterns (discussed later). A ZEISS, SUPRATM 35VP field emission scanning electron microscope (FESEM) was used to analyze the film surface feature and clustered size of ZnO. Transmission electron microscope (TEM) measurement was performed by Tecnai G2 30ST (FEI) electron microscope operating at 300 kV from the scratched off film onto 300 mesh carbon coated cupper grid. The TEM/high resolution TEM (HRTEM) and TEM-energy dispersive spectroscopy

Received: October 24, 2015; **Accepted:** November 14, 2015; **Published:** November 16, 2015

Citation: Pal M, Bera S, Khan H and Jana S * (2015) Effect of Ga doping on Microstructural, Optical and Photocatalytic Properties of Nanostructured Zinc Oxide Thin Films 1:100109

(TEM-EDS) studies were performed for analyses of particle size, crystal phase and tentative content of metals. Surface topography of the films was measured by using atomic force microscope (AFM; Easy Scan 2, Nanosurf AG, Switzerland) and the root mean square (RMS) surface roughness of films were calculated from the AFM surface topography by using a software (WSxM 5.0 Develop 7.0-Image Browser). In this measurement, the dimension along X and Y axes kept fixed for all the films. UV-Vis-NIR spectrophotometer (Shimadzu UV-PC-3100; photometric accuracy: transmission ±0.3%, wavelength resolution, 0.10 nm) was used to measure UV-Vis absorption spectra of the films and the direct band gap energy (BGE) of the samples was determined from the respective film absorption spectrum and film physical thickness using Tauc's equation. A FTIR instrument (Nicolet 5700, USA, wavenumber accuracy: 4 cm^{-1}) was also used for measurement of substrate corrected FTIR vibrations of the films. To measure the photoluminescence property of the films, Perkin-Elmer (LS55) spectrofluorimeter was employed at room temperature. Substrate corrected Raman spectral measurements (micro Raman, Renishaw inVia Raman microscope) was done using argon-ion laser with an incident wavelength of 514 nm as the excitation source at room temperature.

Photocatalytic activity (PA) of the films towards degradation of Rhodamine 6G (Rh-6G) was studied in a custom built stainless steel UV (wavelength, 254 nm) curing chamber. The coated sample (total area, ~3.5 cm^2) was placed nearly 45^o angle with the wall of borosilicate glass beaker of 100 ml capacity containing aqueous solution of dye (10^{-5} M, C_o) using double distilled water. Moreover, the visible photocatalytic activity of a particular film G1ZO was checked under the visible light (source Philips make tungsten bulb, 200 W) exposure using glass filter of 420 nm cut off wavelength. In this respect, the detailed measurement procedure had been reported elsewhere [15]. In a certain time interval, ~4 ml dye solution was taken out and visible absorption spectrum of the solution was recorded to find out the remnant concentration (C) of the dye with the help of a calibration curve of the dye solution. The calibration curve [15,16] was constructed plotting dye concentration against absorbance (OD) at 527 nm peak wavelength of Rh-6G solutions obeying Lambert-Bayer's law. The PA of the films was analyzed by plotting ln (C_o/C) (dye concentration; C_o, initial and C, remnant) versus irradiation time. The degradation rate constant (considering first order reaction kinetics) for each film was determined from the individual plot.

Results and discussion

Phase structure, crystallite size and lattice parameters

X-ray diffraction (XRD) patterns of the films are shown in Figure 1a. The XRD patterns revealed that all the films are nano crystalline in nature and enriched with hexagonal ZnO [h-ZnO, JCPDS Card No. 36-1451]. Moreover, no gallium related crystal or compound was identified [18] from the films within the doping level but the XRD peaks were noticed to be broadened with increasing the doping content, indicating the decrease of crystallite size of ZnO. It is also seen that doping of Ga did not affect the basic crystal structure of ZnO. However, the

Received: October 24, 2015; **Accepted:** November 14, 2015; **Published:** November 16, 2015

Citation: Pal M, Bera S, Khan H and Jana S * (2015) Effect of Ga doping on Microstructural, Optical and Photocatalytic Properties of Nanostructured Zinc Oxide Thin Films 1:100109

crystallite size of ZnO decreased with the doping level. The crystallite size was measured using Scherrer's equation at 2θ angle corresponds to (101) plane of hexagonal ZnO [15,19]. The calculated crystallite size was found to decrease (Fig. 1b) from 9.5 to 7.7 nm (±0.5 nm) with increasing Ga doping level from 0.5 to 6%, respectively. In this respect, it could be noted that the effect of Ga doping on the trend of change of crystallite size of h-ZnO was quite comparable with the Al doped ZnO thin films, reported previously [15]. It is known that the ionic size of Ga (III) (0.62Å) is slightly smaller than that of Zn(II) (0.74 Å) [18]. Therefore, a small amount of gallium could substitute Zn(II) site in ZnO crystal lattice [15,16,20] which would consequence a red shift of 2θ peak in the XRD patterns of the GZO films with respect to the undoped film (G0ZO). This could lead to a change in the lattice parameters (a and c) of the h-ZnO [15,16,21]. We calculated the lattice parameters (a and c) of wurtzite hexagonal ZnO from eqns. 1, 2 and 3 [22,23]. It is to be noted that the XRD peaks for the gallium doped thin films were found to be slightly red shifted up to 1% of Ga doping. This peak shifting would indicate a decrease in lattice parameters (inset, Fig. 1b) which could be due to substitution of Zn (II) by Ga(III) in the ZnO crystal lattice [21]. This result implied that above 1% of Ga doping, the further gallium would not be entered into the Zn(II) site of h-ZnO and it would remain as amorphous phase in the film matrix as no crystalline phase of gallium oxide was detected from the XRD patterns of the films cured at 500°C. The low content of Ga incorporation into the ZnO crystal would be due to self-purification of nanocrystals [10].

$$\frac{1}{d^2} = \frac{4}{3}\left(\frac{h^2+hk+k^2}{a^2}\right) + \frac{l^2}{c^2} \qquad (1)$$

where, d_{hkl} is the interplanar spacing, hkl Miller indices; a, b and c are the lattice parameter of a crystallographic unit cell. The 'a' and 'c' of hexagonal ZnO could be measured from eqns. 2 and 3.

$$\frac{1}{d^2} = \frac{4}{3}\left(\frac{l}{a^2}\right) \qquad (2)$$

$$\frac{1}{d^2} = \frac{4}{c^2} \qquad (3)$$

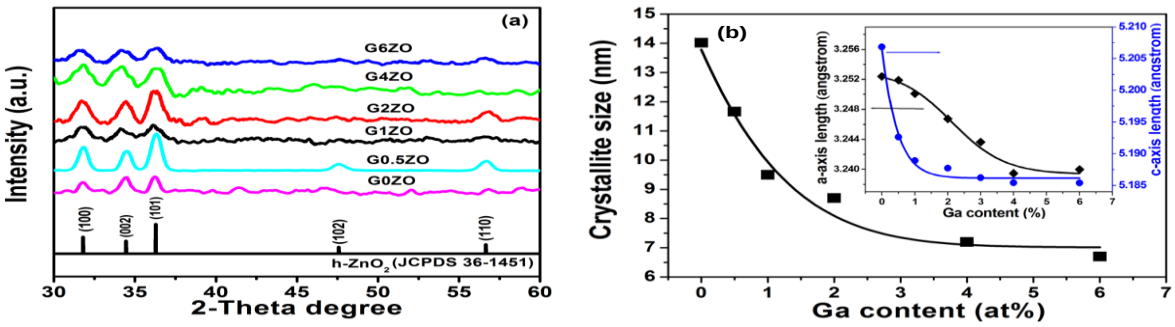

Figure 1: (a) XRD patterns of undoped and Ga doped ZnO thin films. (b) Change of ZnO crystallite size with Ga doping content (inset shows the change in crystal lattice parameters, 'a' and 'c' of hexagonal ZnO as a function of dopant content).

Received: October 24, 2015; **Accepted:** November 14, 2015; **Published:** November 16, 2015

Citation: Pal M, Bera S, Khan H and Jana S * (2015) Effect of Ga doping on Microstructural, Optical and Photocatalytic Properties of Nanostructured Zinc Oxide Thin Films 1:100109

Field emission scanning electron microscopy (FESEM) analysis

The surface feature of ZnO thin films were revealed from FESEM images (Fig. 2). It is observed that irrespective of gallium doping levels, the shape of ZnO clusters remained in spherical shape. Generally, the presence of some anionic impurity like chloride (Cl^-) would influence upon the unequal crystal growth along polar and non-polar surfaces of hexagonal ZnO, would result for the formation hierarchical structures of ZnO such as rods, flowers, petals [19,23] but no such anionic impurity was added in the precursor solutions. This could be a reason for the formation of only spherical shaped ZnO. The cluster size of ZnO calculated from the FESEM images with doping levels 0, 1, 2, 4 and 6 % were ~75, ~ 55, ~ 75, ~ 95 and ~ 110 nm, respectively. Hence, 1% Ga doped G1ZO film showed the lowest clustered size.

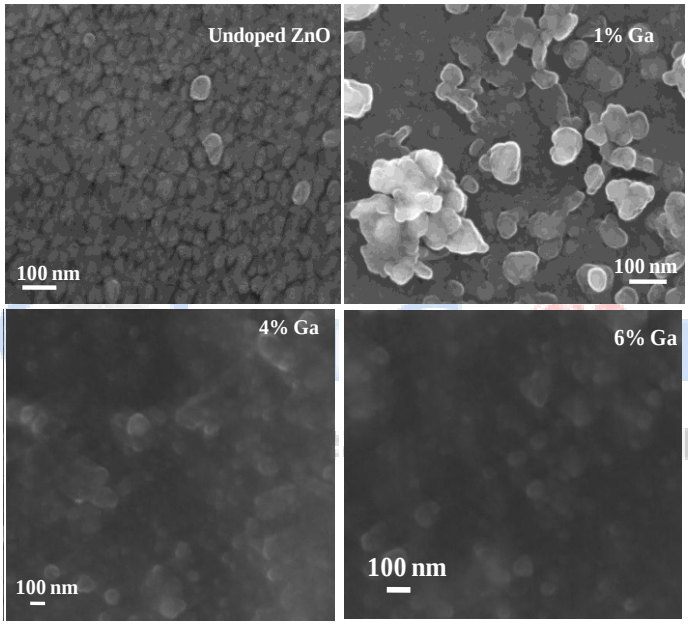

Figure 2: FESEM images of undoped and Ga doped ZnO thin films derived from the solutions of different doping levels.

Transmission electron microscopy (TEM) analysis

TEM result of the films is shown in Figure 3. The particle size of ZnO was calculated from the TEM images (insets, Fig. 3). It is observed that the undoped film (G0ZO) showed quasi-spherical ZnO nano particles with average size ~24 nm whereas the particle size was found to be decreased (~21 nm) in G1ZO and G6ZO films. Hence, the trend in change of particle size as a function of gallium doping level supported the XRD result (Fig. 1). However, the clustered/particle size measured from FESEM/TEM

Received: October 24, 2015; **Accepted:** November 14, 2015; **Published:** November 16, 2015

Citation: Pal M, Bera S, Khan H and Jana S * (2015) Effect of Ga doping on Microstructural, Optical and Photocatalytic Properties of Nanostructured Zinc Oxide Thin Films 1:100109

images was always higher than that of the crystallite size calculated from the XRD patterns. This might be considered due to agglomeration [24] and the agglomeration of particles was seemed to be reduced in the doped films. The EDS (insets (ii), Fig. 3a,c) curves of G0ZO and G6ZO show the presence of Zn, O, C and Cu elements. The source of Zn and O could be from the ZnO films whereas the C and Cu could originate from the carbon coated Cu grids used for the TEM measurement [16]. It is worthy to mention that the high resolution (HRTEM) image of the film also confirmed the presence of hexagonal ZnO (inset ii, Figure. 3b). In this respect, the TEM study strongly supported the XRD result of the films (Figure 1).

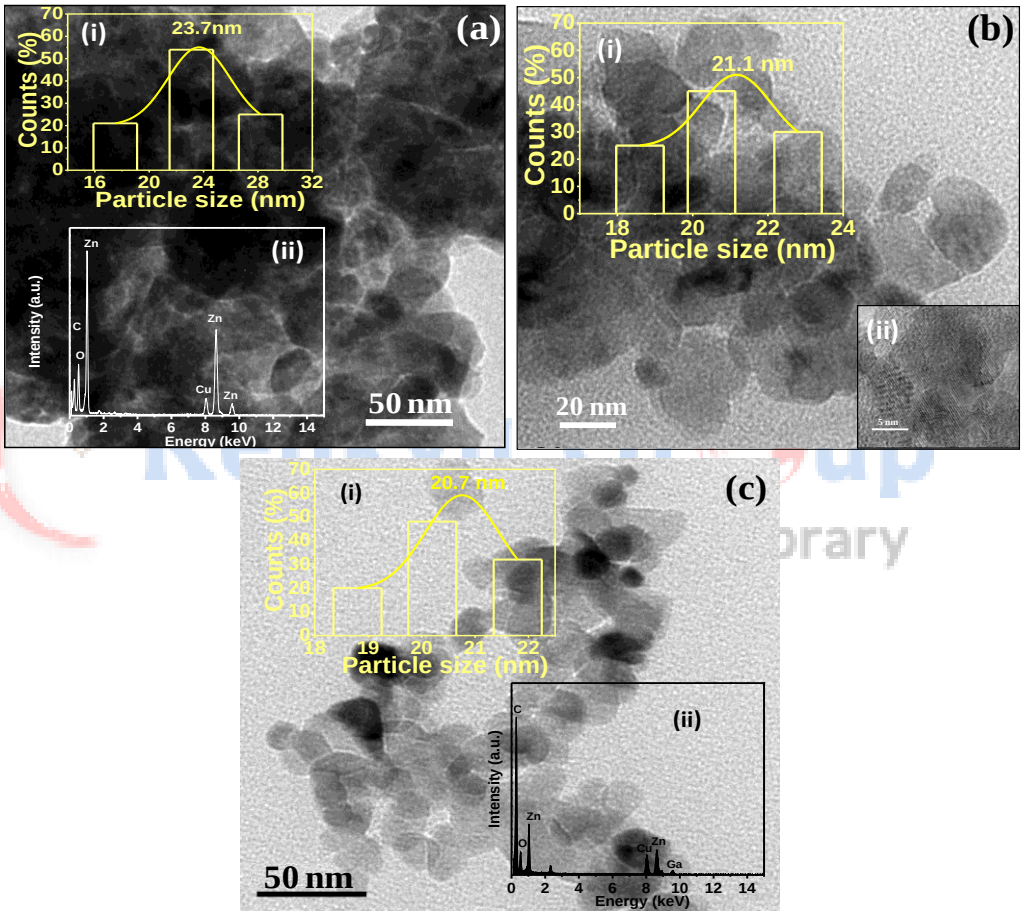

Figure 3: TEM images (a), (b) and (c) of G0ZO, G1ZO and G6ZO, respectively. Insets (i) of (a), (b) and (c) show the histograms for particle size distributions of the respective films. TEM-EDS curves of G0ZO and G1ZO films are also displayed in the insets (ii) of (b) and (c), respectively. HRTEM image (inset (ii) of b) of G1ZO film shows the presence of distinct lattice fringes of hexagonal ZnO nanocrystals.

Received: October 24, 2015; **Accepted:** November 14, 2015; **Published:** November 16, 2015

Citation: Pal M, Bera S, Khan H and Jana S * (2015) Effect of Ga doping on Microstructural, Optical and Photocatalytic Properties of Nanostructured Zinc Oxide Thin Films 1:100109

AFM surface topography and determination of root means square (RMS) surface roughness

Fig. 4 shows the AFM images with RMS surface roughness of different films. The root mean square surface roughness (RMS) was measured from AFM surface topography with an identical X, Y dimensions. It is seen that G1ZO film shows highest RMS surface roughness. It is worthy to note that the trend in change of the roughness as a function of gallium doping content was similar to that of the change of the photocatalytic decomposition rate constant (discussed later).

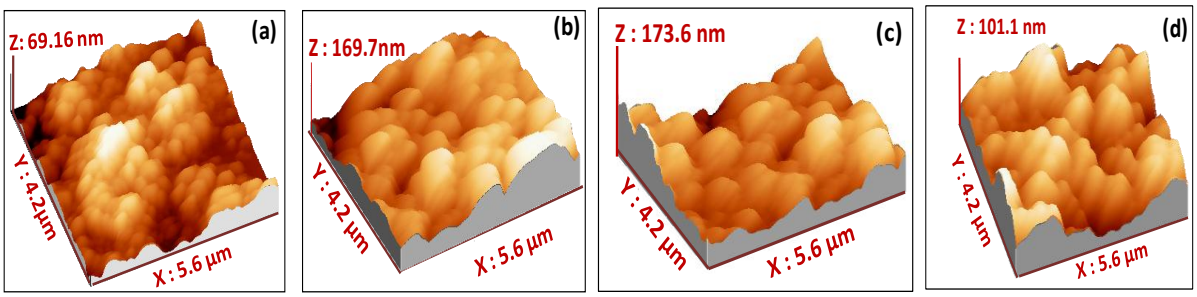

Figure 4: AFM surface topography of (a) G0ZO, (b) G1ZO, (c) G2ZO and (d) G6ZO thin films.

Fourier transform infrared (FTIR) vibrations

Fig. 5 shows substrate corrected FTIR spectra of the films. The FTIR spectra show several absorption peaks within 590-410 cm^{-1}, would responsible due to hexagonal ZnO [25]. In this respect, the FTIR spectra supported the XRD (Fig. 1a) and TEM (Fig. 3) analyses. It is further noted that a distinct vibration at ~640 cm^{-1} that started to appear in G2ZO film and became very strong in G6ZO film. This vibration could be assigned to the asymmetric stretching vibration of Ga-O bond [26]. Thus, it could be considered that the excess gallium would form an amorphous Ga-O network in ZnO grain boundary and would prevent the crystal growth of ZnO [15,27] in the higher doping level of Ga.

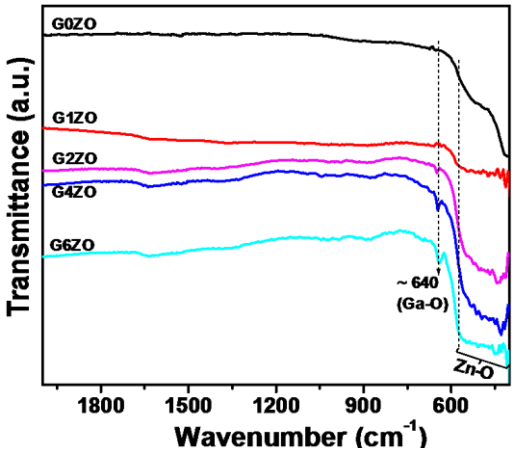

Figure 5: Substrate corrected FTIR spectra of undoped and Ga doped ZnO thin films.

Received: October 24, 2015; **Accepted:** November 14, 2015; **Published:** November 16, 2015

Citation: Pal M, Bera S, Khan H and Jana S * (2015) Effect of Ga doping on Microstructural, Optical and Photocatalytic Properties of Nanostructured Zinc Oxide Thin Films 1:100109

UV-Vis absorption spectra and direct band gap energy

UV-Vis absorption spectra of the GZO films are displayed in Figure 6a. From the absorption spectra, it is seen that there is a broad absorption peak (A) in the UV region and the intensity of the UV peak is also differed in the absorption spectra of the films. Moreover, there is a slight peak shifting as observed from the absorption spectra. Anyhow, the UV absorption would be a characteristic of ZnO semiconductor, could originate due to electron transition from the highest occupied molecular orbital (HOMO) to lowest unoccupied molecular orbital (LUMO) [28] in ZnO molecule and the shifting of A would relate to the change in particle size of ZnO [7,15]. However, the change of intensity of the absorption peak would relate to the difference in film physical thickness.

The shifting of UV absorption peak could clearly be understood from the determination of direct band gap energy (E_g) of the films. Therefore, we calculated the E_g of the films using Tauc's equation [7,16]. It is known that the direct band gap energy (E_g) and the absorption co-efficient (α) are interrelated to each other for direct transition semiconductor like ZnO. The determination of direct band gap energy plots [$(\alpha h\nu)^2$ versus $h\nu$] of the films are shown in Figure 6b,c,d,e. It is worthy to note that in each plot of the film there are two E_g values, one at 3.30 eV which remains approximately same for all the films but another E_g value is found to be increased with increasing Ga doping level. The first one could relate to the bulk band gap energy of ZnO whereas the second one could be due to the size effect of ZnO in the nano regime. It is seen that the calculated E_g values increased at up to 1% Ga doping and it remained approximately same on further increase of the doping content. This could be related to the size effect of nano ZnO [7,29] as evident from the XRD (Figure.1), FESEM (Figure. 2) and TEM (Figure. 3) analyses.

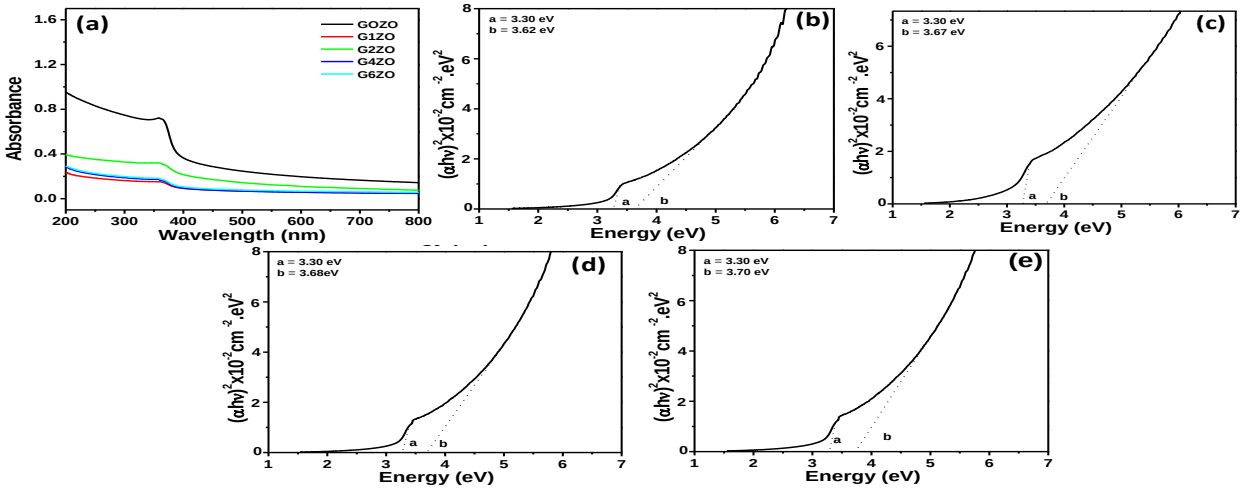

Figure 6: (a) Shows the UV-Vis spectra of undoped and Ga doped films. Determination of direct band gap energy of the films: (a) GOZO, (b) G1ZO, (c) G4ZO and (d) G6ZO.

Received: October 24, 2015; **Accepted:** November 14, 2015; **Published:** November 16, 2015

Citation: Pal M, Bera S, Khan H and Jana S * (2015) Effect of Ga doping on Microstructural, Optical and Photocatalytic Properties of Nanostructured Zinc Oxide Thin Films 1:100109

UV-Vis photoluminescence (PL) emission spectra

The UV-Vis PL spectra (Fig. 7) of the films were measured by fixing the excitation wavelength at 340 nm. The undoped ZnO film (G0ZO) showed PL emissions (inset, Fig. 7) at ~ 398 nm (prominent shoulder), ~ 425 nm, ~ 450 nm, ~ 485 nm and ~ 530 nm. The emission peak appeared at 398 nm could be due to singly negatively charged oxygen vacancy [15]. Generally, five intrinsic defects (oxygen and zinc interstitial, oxygen and zinc vacancies and antisite oxygen) [11] could form within the band gap of ZnO which would able to generate PL emissions after excitation with photons. However, the formation of these defects was dependent on several factors including preparative methods [7,11,15] and doping [12]. In the present work, single ionized (singly positively charged) oxygen vacancy (V_o^+) in the films was characterized from the appearance of PL emission within 450-460 nm [30]. The presence of zinc interstitial (Zn_i) [11] was also supported from the PL emission appeared at 425-430 nm. Moreover, neutral oxygen vacancy would be formed in the film because a prominent emission was observed at 530 nm [31,32]. Also, the formation of antisite oxygen would support by the emission appeared at 485 nm and the combination of electrons between the antisite oxygen and the conduction band might be its origin. It should mention that the position of some other PL peaks observed in the visible region was noticed to slight shift in red/blue wavelength region. This peak shifting would relate with the change in concentration of the defect [33]. In case of G1ZO, G2ZO and G4ZO films, a UV emission peak appeared at ~380 nm would be responsible for the radiative recombination (band edge emission) of the electrons in the conduction band with the holes in the valence band [9] of ZnO semiconductor. However, the UVPL peak was found to be red shifted in G6ZO. It is known that both the particle size of a semiconductor and its surface states would influence on the PL emission. Generally, with decreasing the particle size, the UVPL peak should shift to the shorter wavelength region. Therefore, the UVPL peak shifting in G6ZO film was not according to the particle size change as observed in XRD (Fig.1) and TEM (Fig. 3) results. Therefore, it would be related to the surface states of the ZnO [34]. However, except G0ZO film which possessed intrinsic defects including a singly negatively charged oxygen vacancy due to the appearance of prominent shoulder at ~ 398 nm, the relative intensity of the UV PL was found minimum in G1ZO film, implying that the recombination rate of photogenerated charge carriers (electron and hole) was lowest in this film. Perhaps, the factor that could responsible for inhibition of the photogenerated charge carrier recombination would result in the lowest UVPL intensity in G1ZO film. This would be due to formation of greater number of defects such as oxygen vacancies [15,16,35] in the film network. The matter was studied by Raman spectra (Fig. 8) for evaluation of relative defect concentration in GZO films. This defect could primarily act as electron/hole sink and would consequence a suppression of electron hole recombination [15,35]. Therefore, the PL spectral result, particularly for G1ZO film would be very much useful for enhancing the film photocatalytic activity towards decomposition of an organic dye (rhodamine 6G) under light irradiation (discussed later on).

Received: October 24, 2015; **Accepted:** November 14, 2015; **Published:** November 16, 2015

Citation: Pal M, Bera S, Khan H and Jana S * (2015) Effect of Ga doping on Microstructural, Optical and Photocatalytic Properties of Nanostructured Zinc Oxide Thin Films 1:100109

Raman spectral analysis

ZnO is an n-type semiconductor as it inherently possesses natural oxygen vacancy [12]. The defect concentration could be controlled by incorporation of dopant such as Al into the ZnO crystal lattice [15]. In the periodic table of elements, gallium belongs to the same group (Group IIIA) of B and Al. Therefore, incorporation of gallium into the ZnO lattice site, there could be a change in concentration of the defect depending upon the Ga doping level. The equation for different optical phonon vibrations in the hexagonal wurtzite ZnO crystal at the Γ -point could be expressed by an irreducible representation (eqn. 4).

$$\Gamma = A_1 + 2B_1 + E_1 + 2E_2 \quad (4)$$

In equation (4), both A_1 and E_1 modes are Raman and IR active whereas the E_2 mode is only Raman active whereas B_1 is known to be forbidden. Moreover, the E_1 mode could split into transverse optical (TO) and longitudinal optical (LO) components. Raman spectra of G0ZO, G1ZO, G2ZO and G4ZO

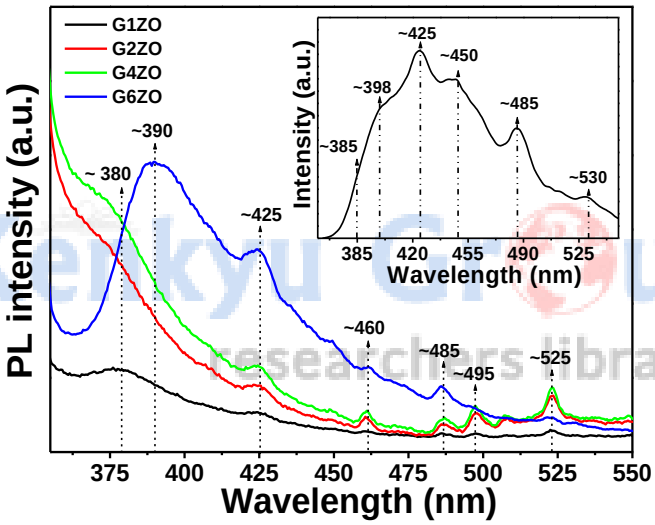

Figure 7: Photoluminescence (PL) emission spectra (λ_{ex} = 340 nm) of undoped and Ga doped films (inset shows the PL spectrum of B0ZO film).

films are shown in Figure. 8a. In the undoped and doped films, three Raman peaks appeared at 329 cm-1 [medium intensity, assigned to TO-TA(M)] [15] along with 437 and 582 cm^{-1}. The Raman peak appeared at 437 cm^{-1} could indicate the characteristic Raman vibration of wurtzite hexagonal ZnO crystal in E_2(high) mode [7,15] whereas the E_1(LO) peak at 582 cm^{-1} would relate to the defect (oxygen vacancy) [7] present in the nanostructured ZnO film. In this respect, the change of intensity ratio (R), E_1(LO) / E_2(high) could be an useful tool to determine the variation in defect concentration of hexagonal ZnO and the value R could show the relative defect concentration. We calculated R values of 0.985, 1.1,

Received: October 24, 2015; **Accepted:** November 14, 2015; **Published:** November 16, 2015

Citation: Pal M, Bera S, Khan H and Jana S * (2015) Effect of Ga doping on Microstructural, Optical and Photocatalytic Properties of Nanostructured Zinc Oxide Thin Films 1:100109

1.25, 0.581 and 0.287 for the films G0ZO, G0.5ZO, G1ZO, G2ZO and G4ZO, respectively. The R values were plotted against the doping content (Fig. 8b). The plot shows that the G1ZO film possessed the maximum defect concentration (oxygen vacancy) within the experimental doping level. It is worthy to note that the trend of change in defect concentration with respect to Ga doping level was also found to be identical with the change of photocatalytic activity in terms of dye decomposition rate constant (Fig. 8b) of the films (discussed later) .

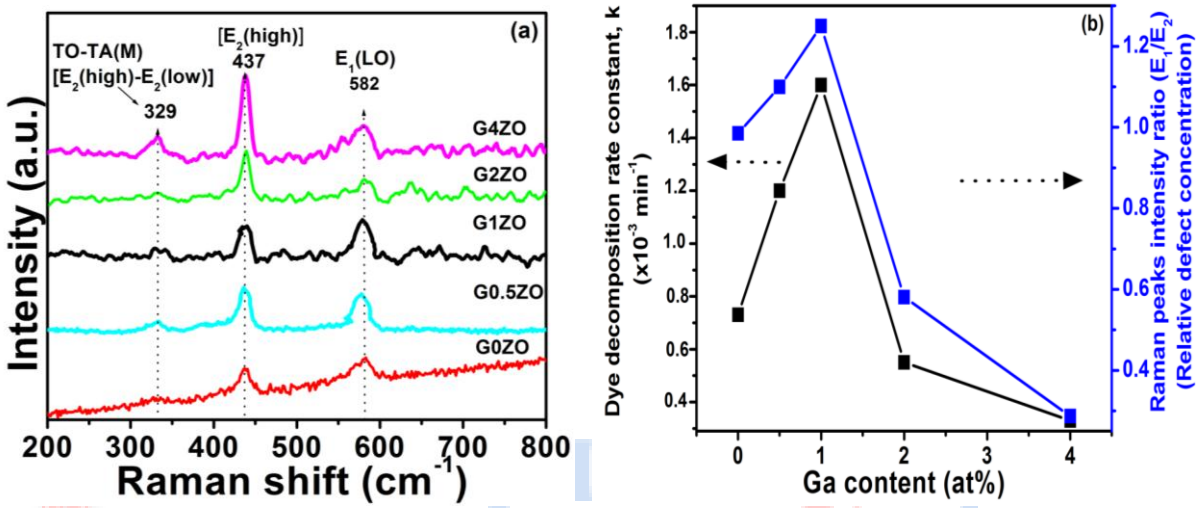

Figure 8: (a) Substrate corrected Raman spectra of undoped and Ga doped ZnO films; (b) Plots show the change of defect concentration of the films calculated from Raman spectral analysis (intensity ratio of Raman peaks, E_1/E_2) and the first order dye decomposition rate constant under UV exposure against Ga doping level.

Photocatalytic activity

Photodecomposition study (Figures. 9, 10) was performed on aqueous Rh-6G dye solution (10^{-5} M) in presence of the Ga doped ZnO thin films as photocatalysts under UV (λ, 254 nm). Moreover, the photocatalytic activity of G1ZO film which possessed highest defect concentration was checked under visible light irradiation. Under the UV light, the dye decomposition rate constant (considering the first order reaction kinetics), k ($x10^{-3}$) values were 0.74, 1.20, 1.60, 0.55, 0.33, and 0.12 min^{-1} for the films, G0ZO, G0.5ZO, G1ZO, G2ZO, G4ZO and G6ZO, respectively whereas the k value for the G1ZO film obtained under visible light was $1.08x10^{-3}$ min^{-1}. Thus, in the present work, the highest k value was found in 1% Ga doped zinc oxide (G1ZO) and the G6ZO film showed the lowest 'k' value under UV irradiation.

Received: October 24, 2015; **Accepted:** November 14, 2015; **Published:** November 16, 2015

Citation: Pal M, Bera S, Khan H and Jana S * (2015) Effect of Ga doping on Microstructural, Optical and Photocatalytic Properties of Nanostructured Zinc Oxide Thin Films 1:100109

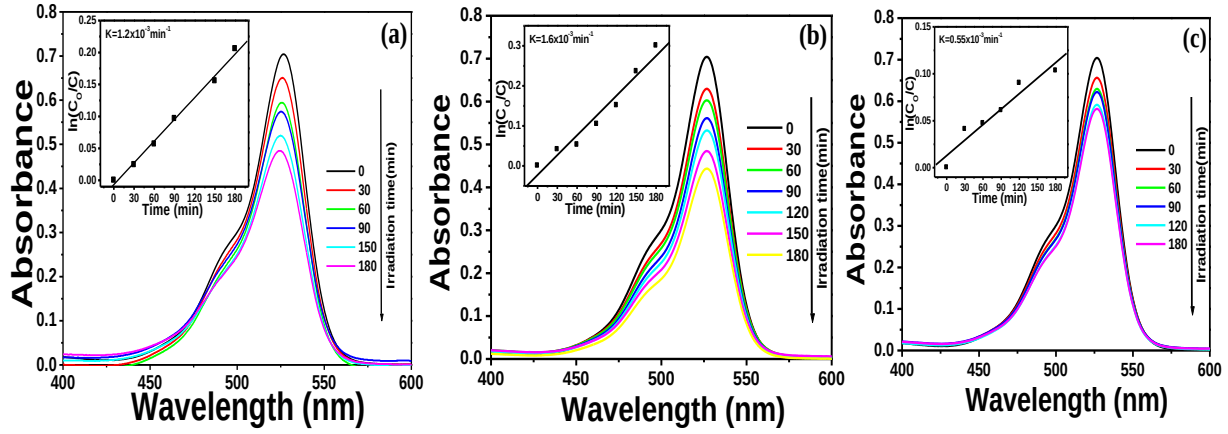

Figure 9: (a), (b) and (c) show the UV-Vis spectra of the dye (Rh-6G) at different time of UV (λ = 254 nm) irradiation using the photocatalysts, G0.5ZO, G1ZO and G2ZO, respectively. Insets show the determination of first order rate constant 'k' of the dye photodecomposition reaction.

Correlation of different properties to photocatalytic activity of the films

Generally, the photocatalytic activity of metal oxide semiconductor film depends upon various parameters [15,16,19] such as particle size (inversely related to band gap energy) and surface area (inversely proportional to particle size), surface roughness, defect concentration etc. In the present work, the particle size of ZnO vis-a-vis the band gap energy of the films systematically decreased with increasing Ga doping content as confirmed from the XRD (Fig. 1) and TEM (Fig. 3) analyses. Therefore, the change of crystallite/particle size vis-a-vis the band gap value of the films was not the factors to explain the photocatalytic activity of the films. However, the defect concentration especially the presence of oxygen vacancies determined from the Raman spectral analysis (Fig. 8b) was found to be systematically increased up to 1% of Ga doping and then, it was decreased on further increase of the doping level. It is also important to mention that the trend in change of defect concentration was found to be similar with the change of k value of the photocatalyst film as a function of doping level. In this respect, several defects (such as oxygen vacancies, zinc interstitials etc.) were characterized from the photoluminescence (PL) spectral study (Fig. 7) of the films. Moreover, the maximum RMS surface roughness value was found in G1ZO film. This could be an advantageous factor for the enhancement of PA. This is because more surface roughness would increase the number of available surface sites which could enhance the contact of dye molecule with the photocatalyst [14]. This would result an improvement of the photocatalytic activity [14] of the film. Therefore, the synergic effect of maximum relative defect concentration as well as the surface roughness parameters of G1ZO could play the roles in G1ZO film to enhance its photocatalytic activity without adding the individual contribution of the parameters i.e. the defect concentration and

Received: October 24, 2015; **Accepted:** November 14, 2015; **Published:** November 16, 2015

Citation: Pal M, Bera S, Khan H and Jana S * (2015) Effect of Ga doping on Microstructural, Optical and Photocatalytic Properties of Nanostructured Zinc Oxide Thin Films 1:100109

surface roughness. In this respect, we had checked the PA of G1ZO under visible light exposure and found an appreciable value of k ($1.08x10^{-3}$ min^{-1}). Therefore, the defect concentration was found to be influenced greatly than the surface roughness with respect to the photocatalytic activity of the films. On the other hand, the presence of amorphous gallium oxide as revealed by the observation of a strong Ga-O FTIR vibration (Fig. 5) in the film would be a reason for the lowest value of k in G6ZO film because the amorphous Ga oxide would cover the active sites of nanocrystalline ZnO photocatalyst and would decrease the possibility of direct contact of the dye molecules with the photocatalyst surface as a result the PA would be reduced remarkably [15,27].

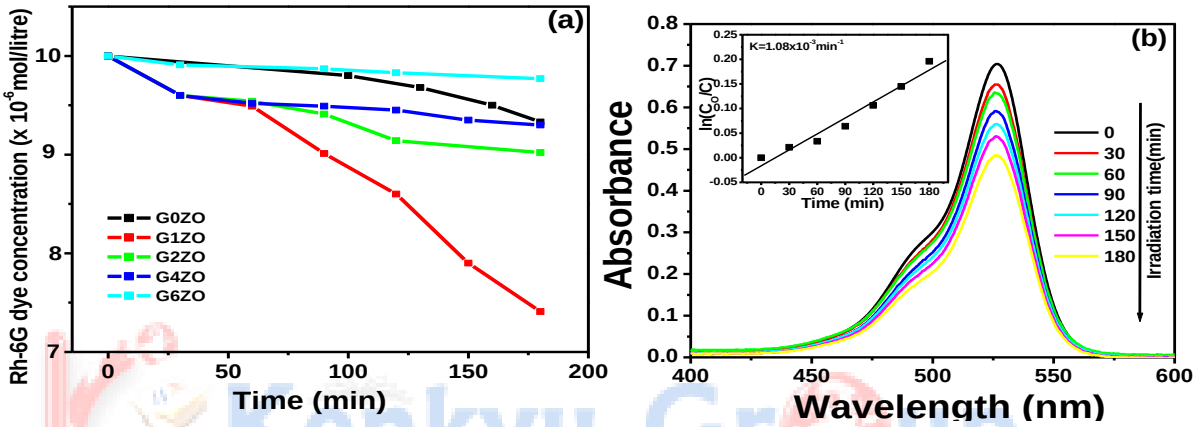

Figure 10: (a) Plots of remnant dye concentration of Rh-6G dye at different time of UV exposure using the ZnO thin films as photocatalysts. (b) Shows the UV-Vis spectra of the dye (Rh-6G) at different time of visible light exposure using G1ZO film as photocatalyst (inset, determination of first order rate constant 'k' of the photodecomposition of Rh-6G).

Conclusions

In summary, Ga doped nanostructured zinc oxide thin films on pure silica glass substrate were prepared from zinc acetate based precursor solutions by varying Ga doping level (0 to 6%). The presence of quasi-spherical nanocrystalline hexagonal ZnO with a decreased trend in crystallite/particle size vis-à-vis an enhancement of direct band gap energy of the films found on increasing the doping level. Root means square (RMS) film surface roughness was found maximum in 1% doped film (G1ZO). Photoluminescence (PL) emission study revealed that the formation of various intrinsic/extrinsic defects along with the presence of characteristics band edge emission of ZnO at ~ 385 nm (UVPL) and a lowest relative intensity of the UVPL emission was found in 1% doped film (G1ZO), indicating an appreciable decrease in the recombination rate of photogenerated charge carriers in the semiconductor. The photocatalytic activity (PA) of the films towards degradation of rhodamine 6G dye was performed under UV (254 nm) and obtained the maximum value of dye degradation first order reaction rate constant in 1% doped film. On increasing doping level, the trend

Received: October 24, 2015; **Accepted:** November 14, 2015; **Published:** November 16, 2015

in change of defect concentration (oxygen vacancies) as analyzed by Raman spectra was found identical with the dye photodegradation activity of the films. Thus, a synergic effect of the maximum RMS surface roughness and the maximum defect concentration in G1ZO film could be responsible for its highest PA. The G1ZO film would expect to decompose micro-organisms even under exposure of visible light.

Acknowledgements

The authors wish to acknowledge the Director, CSIR-CGCRI, Kolkata for his encouragement. The authors (MP and SB) thank University Grant Commission (UGC) and Council of Scientific and Industrial Research (CSIR), Govt. of India, respectively for providing their research fellowships. The authors also acknowledge the help rendered by Nanostructured Materials Division, Advanced Mechanical and Material Characterization Division and Advanced Material Characterization Unit for several characterizations of samples. The work has been done as an associated project work under CSIR funded Supra Institutional Network Project (SINP) (No. ESC0202) of 12th Five Year Plan.

References

1. Hoffmann MR, Martin ST, Choi W, Bahnemann DW (1995) Environmental applications of semiconductor photocatalysis. Chem. Rev. 95: 69-96.
2. Kim CE, Moon P, Yun I, Kim S, Myoung JM, et al. (2011) Process estimation and optimized recipes of ZnO:Ga thin film characteristics for transparent electrode applications. Expert Systems Appl. 38: 2823–2827.
3. Rusu GG, Rambu AP, Buta VE, Dobromir M, Luca D, Rusu M (2010) Structural and optical characterization of Al-doped ZnO films prepared by thermal oxidation of evaporated Zn/Al multilayered films. Mater. Chem. Phys. 123: 314–321.
4. Zainullina VM, Zhukov VP, Korotin MA, Polyakov EV (2011) Effect of doping by boron, carbon, and nitrogen atoms on the magnetic and photocatalytic properties of anatase. Phys. Solid State 53: 1353–1361.
5. Tewari S and Bhattacharjee A (2011) Structural, electrical and optical studies on spray-deposited aluminium-doped ZnO thin films. Pramana– J. Phys. 76: 153–163.
6. Shui A, Wang S, Wang H, Cheng X (2009) Preparation and properties for Al doped ZnO powders with the coprecipitation method. J. Ceram. Soc. Jpn 117: 703–705.
7. Jana S, Vuk AS, Mallick A, Orel B, Biswas PK (2011) Effect of boron doping on optical properties of sol–gel based nanostructured zinc oxide films on glass. Mater. Res. Bull. 46: 2392–2397.
8. Likovich EM, Jaramillo R, Russell KJ, Ramanathan S, Narayanamurt V (2011) Narrow band defect luminescence from Al-doped ZnO probed by scanning tunneling cathodoluminescence. Appl. Phys. Lett. 99: 151910 (3 pages)
9. Pradhan P, Alonso JC, Bizarro M (2012) Photocatalytic performance of ZnO: Al films under different light sources. Int. J. Photoenergy 2012: 780462 (7 pages).

Received: October 24, 2015; **Accepted:** November 14, 2015; **Published:** November 16, 2015

10. Dalpian GM, Chelikowsky JR (2006) Self-purification in semiconductor nanocrystals. Phys. Rev. Letts 96: 226802 (4 pages).
11. Zhao L, Lian JS, Liu Y, Jing Q (2008) Influence of preparation methods on photoluminescence properties of ZnO films on quartz glass. Trans. Nonferrous Met. Soc. China 18: 145–149.
12. Kung CY, Young SL, Chen HZ, Kao MC, Horng L, et al. (2012) Influence of Y-doped induced defects on the optical and magnetic properties of ZnO nanorod arrays prepared by low-temperature hydrothermal process. Nanoscale Res. Letts. 7: 372 (6 pages).
13. Wang J, Liu P, Fu X, Li Z, Han W, et al. (2009) Relationship between oxygen defects and the photocatalytic property of ZnO nanocrystals in nafion membranes. Langmuir 25: 1218-1223.
14. Moore JC, Louder R, Thompson CV (2014) Photocatalytic activity and stability of porous polycrystalline ZnO thin-films grown via a two-step thermal oxidation process. Coatings 4: 651–669.
15. Pal M, Bera S, Sarkar S and Jana S (2014) Influence of Al doping on microstructural, optical and photocatalytic properties of sol–gel based nanostructured zinc oxide films on glass. RSC Adv. 4: 11552–11563.
16. Pal M, Bera S and Jana S (2013) Effect of precursor sol pH on microstructural, optical and photocatalytic properties of vacuum annealed zinc tin oxide thin films on glass. J Sol-Gel Sci Technol 67: 8–17.
17. Lalanne M, Soon JM, Barnabe A, Presmanes L, Pasquet I, et al. (2010) Preparation and characterization of the defect–conductivity relationship of Ga-doped ZnO thin films deposited by nonreactive radio-frequency–magnetron sputtering. J. Mater. Res. 25: 2407–2414.
18. Wei H, Li M, Ye Z, Yang Z, Zhang Y (2011) Novel Ga-doped ZnO nanocrystal ink: synthesis and characterization. Mater. Lett. 65: 427–429.
19. Bera S, Pal M, Sarkar S, Jana S (2013) Dependence of precursor composition on patterning and morphology of sol–gel soft lithography based zinc zirconium oxide thin films. Appl. Surf. Sci. 273: 39–48.
20. Xue Y, He H, Jin Y, Lu B, Cao H, et al. (2014) Effects of oxygen plasma treatment on the surface properties of Ga-doped ZnO thin films. Appl. Phys. A 114: 509–513.
21. Jun MC, Park S-U, Koh JH (2012) Comparative studies of Al-doped ZnO and Ga-doped ZnO transparent conducting oxide thin films. Nanoscale Res. Lett. 7: 639 (6 pages)
22. AR (2014) Solid State Chemistry and its Applications. (2nd edn.), Wiley.
23. Mohammad RA, Henley SJ, Emerson NG, Silva SRP (2014) From 1D and 2D ZnO nanostructures to 3D hierarchical structures with enhanced gas sensing properties. Nanoscale 6: 235-247.
24. Joshi R, Waldschmidt B, Engstler J, Schäfer R, Schneider JJ (2011) Generation and agglomeration behaviour of size-selected sub-nm iron clusters as catalysts for the growth of carbon nanotubes. Beilstein J Nanotechnol 2: 734–739.

Received: October 24, 2015; **Accepted:** November 14, 2015; **Published:** November 16, 2015

25. Kolev G, Aleksandrova M, Vucheva Y, Denishev K (2014) Thin film microsensing elements, technology and application in microsystems for environment control. J. Phys. Conf. Series 559: 012015 (6 pages).
26. Ristic M, Popovic TS, Music S (2005) Application of sol–gel method in the synthesis of gallium (III)-oxide. Mater. Lett. 9: 1227–1233.
27. Hu S, Nozawa J, Koizumi H, Fujiwara K, Uda S (2015) Grain boundary segregation of impurities during polycrystalline colloidal crystallization. Cryst. Growth. Des. DOI: 10.1021/acs.cgd.5b00646.
28. Wadeasa A (2011) Heterojunctions between zinc oxide nanostructures and organic semiconductor. Linkoping Studies in Science and Technology. Dissertations, No. 1405 ISSN: 0345–7524.
29. Lin H, Huang CP, Li W, Ni C, Shah SI, et al. (2006) Size dependency of nanocrystalline TiO_2 on its optical property and photocatalytic reactivity exemplified by 2-chlorophenol. Appl. Catal. B Environ. 68: 1–11.
30. Gao M, Yang J, Yang L, Zhang Y, Lang J, et al. (2012) Enhancement of optical properties and donor-related emissions in Y-doped ZnO. Superlattice Microstructure 52: 84–91.
31. Ye D, Gu SL, Zhu SM, Qin F, Liu SM, et al. (2004) Production of high-quality ZnO films by the two-step annealing method. J. Appl. Phys. 96: 5308-5310.
32. Willander M, Nur O, Sadaf JR, Qadir MI, Zaman S, et al. (2010) Luminescence from zinc oxide nanostructures and polymers and their hybrid devices. Materials 3: 2643–2667.
33. Kondela T, Gregus J, Zahoran M, Roch T (2010) Energy shift of native 2.45 eV related defects in annealed ZnO Films. IOP Conf. Series Mater. Sci. Eng. 15: 012041 (7 pages).
34. Yang Z (2008) Preparation of palladium, palladium sulfide, cadmium selenide nanoparticles and magnesium oxychloride, magnesium hydroxide nanorods. Kansas State University, Manhattan, Kansas, Ph.D. Dissertation, Chapter 5.
35. Liquiang J, Yichun Q, Baiqui W, Shudan L, Baojiang F, et al. (2006) Review of photoluminescence performance of nano-sized semiconductor materials and its relationships with photocatalytic activity. Sol. Eng. Mater. Sol. C. 90: 1773–1787.

Received: October 24, 2015; **Accepted:** November 14, 2015; **Published:** November 16, 2015